Archivum Immunologiae et Therapiae Experimentalis (2023) 71:20
https://doi.org/10.1007/s00005-023-00685-w

ORIGINAL ARTICLE

Improved Production of Anti-FGF-2 Nanobody Using *Pichia pastoris* and Its Effect on Antiproliferation of Keratinocytes and Alleviation of Psoriasis

Zhenlong Zhou[1,2] · Baixin Liao[1] · Shengli Wang[3] · Jian Tang[1] · Hui Zhao[1] · Mingjie Tong[1] · Keting Li[1] · Sheng Xiong[1]

Received: 20 March 2023 / Accepted: 14 July 2023 / Published online: 26 August 2023

Abstract

Fibroblast growth factor 2 (FGF-2) is not only an angiogenic factor, but also a mitogen for epidermal keratinocytes. FGF-2 has been shown to be positively immunoreactive in the basal layer of psoriatic lesions. In previous work, we used the *Escherichia coli* (*E. coli*) expression system to biosynthesize a biologically active anti-FGF-2 nanobody (Nb) screened by phage display technology, but the low yield limited its clinical application. In this study, we aimed to increase the yield of anti-FGF-2 Nb, and evaluate its therapeutic potential for psoriasis by inhibiting FGF-2-mediated mitogenic signaling in psoriatic epidermal keratinocytes. We demonstrated a 16-fold improvement in the yield of anti-FGF-2 Nb produced in the *Pichia pastoris (P. pastoris)* compared to the *E. coli* expression system. In vitro, the FGF-2-induced HaCaT cell model (FHCM) was established to mimic the key feature of keratinocyte overproliferation in psoriasis. Anti-FGF-2 Nb was able to effectively inhibit the proliferation and migration of FHCM. In vivo, anti-FGF-2 Nb attenuated the severity of imiquimod (IMQ)-induced psoriatic lesions in mice, and also improved the inflammatory microenvironment by inhibiting the secretion of inflammatory cytokines (IL-1β, IL-6, IL-23, and TNF-α), chemokines (CXCL1 and CCL20), and neutrophil infiltration in skin lesions. These were mainly related to the suppression of FGF-2-mediated mitogenic signaling in psoriatic keratinocytes. In conclusion, we have improved the production of anti-FGF-2 Nb and demonstrated the modality of attenuating the abnormal proliferative behavior of psoriatic keratinocytes by inhibiting FGF-2-mediated mitogenic signaling, which offers the possibility of treating psoriasis.

Keywords Psoriasis · FGF-2 · Nanobody · *Pichia pastoris* · HaCaT cells · Psoriasis-like mice

Introduction

Psoriasis is a chronic inflammatory skin disease that is polygene-associated and immune-mediated (Armstrong and Read 2020). Its main pathogenesis involves the dysregulation of the interaction between immune cells, epidermal keratinocytes, and endothelial cells, leading to hyperkeratosis and vascularization in psoriatic lesions (Gao et al. 2020). To date, there is no complete cure for psoriasis. Although drugs with extensive clinical experience such as methotrexate, cyclosporine, and oral retinoids are widely used in the treatment of psoriasis, these drugs inevitably have adverse effects on the host tissues (Kormeili et al. 2004). It is therefore imperative to develop a safe and effective drug for the treatment of psoriasis.

Extensive research has been devoted to elucidating the pathogenesis of cytokine-mediated psoriasis. Based on this, significant advances are being made in the treatment of psoriasis through the immune-targeted human cytokine network

Zhenlong Zhou, Baixin Liao and Shengli Wang have contributed equally to this work.

✉ Sheng Xiong
xsh_jnu@hotmail.com

[1] Institute of Biomedicine and National Engineering Research Center of Genetic Medicine, College of Life Science and Technology, Jinan University, Guangzhou 510632, People's Republic of China

[2] School of Food Science and Engineering, South China University of Technology, Guangzhou 510640, People's Republic of China

[3] Institute of Biomedical Transformation, School of Basic Medicine and Public Health, Jinan University, Guangzhou 510632, People's Republic of China

(Landeck et al. 2021). Monoclonal antibodies (mAbs) have played a representative role in these advances, as they can safely and effectively target specific cytokines to achieve various immunotherapeutic effects. The U.S. Food and Drug Administration and the European Medicines Agency have approved tumor necrosis factor (TNF) inhibitor (adalimumab), interleukin (IL)-17 inhibitor (brodalumab), and IL-23 inhibitor (risankizumab) for the treatment of moderate to severe psoriasis patients (Amin et al. 2018; Haugh et al. 2018). However, the development of mAbs is limited by their large molecular weight, high immunogenicity, low stability, and high cost of large-scale production (Battaglin et al. 2019; Paz-Ares et al. 2016; Song et al. 2014; Tol and Punt 2010; Vivanco and Mellinghoff 2010). In contrast, camelid and shark-derived Nbs, variable domains of the heavy chain of heavy-chain antibodies (VHHs), can overcome these limitations. Nbs are relatively stable and easily permeable to tissues due to their small molecular size (2.5 nm × 4 nm × 3 nm) (Kijanka et al. 2015; Wang et al. 2020). In addition, they are typically biosynthesized using engineered *E. coli* and yeast expression systems, making them easy to produce on a large scale at a low cost (Liu et al. 2021). Most importantly, Nbs have low immunogenicity compared to mAbs due to their high homology to the human VH domain and lack of an Fc domain capable of triggering complement responses associated with immunogenicity (Hu et al. 2017; Salvador et al. 2019). These have led to an increasing focus by medical experts on the application of Nbs in clinical practice (Yang and Shah 2020).

FGF-2, a member of the FGF family, plays a critical role in physiological and pathological processes by interacting with cell surface receptors (FGFRs) (Dailey et al. 2005). FGF-2 has been identified as an important target for the treatment of tumors (Wu et al. 2013), but little information is available on its role in the pathogenesis of psoriasis (Chen et al. 2004; Ferrara 1999; Zittermann and Issekutz 2006). Andrys et al. (2007) reported that Goeckerman's therapy significantly reduced angiogenic activity in psoriasis patients by downregulating the expression of the angiogenic factor FGF-2 in serum levels. Importantly, FGF-2 also acts as a keratinocyte mitogen, and its positive immunoreactivity has been observed in the basal layer of psoriatic lesions (Yaguchi et al. 1993), which have a higher mitotic index than healthy skin.

Phage display technology, an important tool in drug discovery, has been widely used to screen for desired Nbs that specifically target specific molecules (Ledsgaard et al. 2022). In previous work, our laboratory successfully used this technology to screen an Nb (F3) that specifically targets FGF-2 and negatively regulates the proliferative process in FGF-2-induced endothelial cells in vitro (Xiong et al. 2022). However, the *E. coli* expression system yielded only about 2.5 mg of purified F3 from 1 L of total induced cell lysates, and the low yield limited its application. Furthermore, the efficacy of using this Nb to treat psoriasis by inhibiting the mitogenic signaling pathway in psoriatic epidermal keratinocytes remains unknown. In this study, we constructed a deglycosylated mutant F3 (M-F3) and expressed it recombinantly in the *P. pastoris* expression system to increase yield. Importantly, we established an in vitro FHCM that mimics overproliferating keratinocytes and used it to assess the anti-proliferative and anti-migratory effects of M-F3. Additionally, we evaluated the effect of M-F3 on IMQ-induced psoriasis-like skin lesions in mice in vivo, and measured proliferation levels, mRNA expression levels of inflammatory cytokines (IL-1β, IL-6, IL-23, and TNF-α) and chemokines (CXCL1 and CCL20), and neutrophil infiltration in skin lesions.

Materials and Methods

Construction of Eukaryotic Expression Plasmid

The cDNA sequence of F3 was reported in our previous study (Xiong et al. 2022). The NetNGlyc 1.0 online server (http://www.cbs.dtu.dk/services/NetNGlyc/) was used to determine the putative N-glycosylation sites in the F3 amino acid sequence. The putative N-glycosylation site (asparagine, N) at position 25 in the F3 amino acid sequence was replaced by glutamine (Q) to construct the M-F3. The cDNA sequence encoding M-F3 was fused to a 6 × His tag at the C-terminus and synthesized by Sango Biotech (Shanghai, China) for the construction of recombinant pPICzα A-M-F3 plasmid.

Expression of Recombinant M-F3

Twenty μg of recombinant pPICzα A-M-F3 plasmid was digested using QuickCutTM Sac I (Takara, Japan). The linearized DNA fragments were purified using the cyclepure kit (Omega Bio-Tek, USA). After purification, 5 μg of linearized DNA fragments were transformed with GS115 strains according to the manufacturer's instructions (Pyt Bio, China). The mixture was then plated on YPD solid plates (HKM, China) containing 2 mg/mL zeocin for 3 days to form cell clones. Positive transformants were identified by colony polymerase chain reaction (PCR). Individual positive transformants were inoculated into YPD medium (HKM, China) in a shaking incubator (220 rpm) at 30 °C for 16–20 h. After incubation, the cell cultures were further inoculated into BMGY medium (Sango Biotech, China) at a volume ratio of 1:100. At an OD_{600} of approximately 2–5, the cell cultures were centrifuged for 5 min to collect the cell precipitates. The cell precipitates were then diluted with BMMY medium (Sango Biotech, China) containing

0.05% methanol to an OD_{600} of 1 for incubation at 28 °C in a shaking incubator (220 rpm) for 120 h. Methanol was added every 24 h to a final concentration of 0.5%.

Purification of Recombinant M-F3

The secreted supernatant containing recombinant M-F3 was loaded onto Ni–NTA agarose (GE, USA). The recombinant M-F3 and some endogenous yeast host proteins were eluted using phosphate buffer saline (PBS, pH 7.4) containing 0–300 mM imidazole. The eluted fraction was analyzed by sodium dodecyl sulfate–polyacrylamide gel electrophoresis (SDS-PAGE) followed by Coomassie brilliant blue staining. The final yield of M-F3 was quantified using the BCA protein assay kit (ThermoFisher, USA).

N-glycosylation Detection

Recombinant F3 (*P. pastoris*) was prepared with reference to M-F3. Ten μg of purified F3 and M-F3 were incubated with or without 1 μL of peptide N-glycosidase F (PNGase F, Merck, Germany) at 37 °C for 24 h. The mixture was subjected to SDS-PAGE followed by Coomassie brilliant blue staining to verify the presence of N-glycosylation sites in the amino acid sequence of M-F3.

SDS-PAGE and Immunoblotting

One hundred μL of electrophoresis samples containing 80 μL of protein samples and 20 μL of 5 × SDS-PAGE sample loading buffer (Beyotime, China) were boiled for 10 min. After 15% reducing SDS-PAGE, the gels were stained and destained with Commassie blue staining reagent (Solarbio, China). The gels were then photographed using a Gel DocTM XR + (Bio-Rad, USA). Proteins from the gels were transferred to 0.45 μm nitrocellulose (NC) membrane (Merck, Germany) for immunoblotting. After treatment with blocking buffer (Solarbio, China), the NC membrane was incubated with horseradish peroxidase (HRP)-conjugated mouse anti-His antibody (Proteintech, China) at 37 °C for 4 h. Immunoreactive bands were exposed to enhanced chemiluminescence (ECL, Yeasen, China) and visualized with Gel DocTM XR+.

ELISA Assay

Briefly, FGF-2, FGF-1, KGF, EGF, Her-2, BSA, and milk were dissolved in coating buffer (Solarbio, China) to a final concentration of 0.5 μg/mL and then added to 96-well ELISA plates at 100 μL per well for overnight incubation at 4 °C. After blocking with 5% non-fat milk for 2 h, 300 ng/mL of M-F3 or PBS used as a blank control was added to each well separately for 1 h incubation at 37 °C. After incubation with HRP-conjugated mouse anti-His antibody for 1 h at 37 °C, 100 μL of 3,3′,5,5′ tetramethylbenzidine (TMB) color developing solution (Innoreagents, China) was added per well and incubated at 37 °C for 10 min. After termination with 2.29% H_2SO_4, the OD was calculated by subtracting the absorbance value at 630 nm from the absorbance value at 450 nm.

Non-competitive ELISA Assay

Briefly, FGF-2 was dissolved in coating buffer to a final concentration of 2 μg/mL, 1 μg/mL, 0.5 μg/mL, and 0.25 μg/mL and then added to 96-well ELISA plates at 100 μL per well for overnight incubation at 4 °C. After blocking with 5% non-fat milk for 2 h, a gradient dilution of M-F3 at a ratio of 4:1 or PBS used as a blank control was added to each well separately for 1 h incubation at 37 °C. After incubation with HRP-conjugated mouse anti-His antibody for 1 h at 37 °C, 100 μL of TMB color developing solution was added per well and incubated for 10 min at 37 °C. After termination with 2.29% H_2SO_4, the OD was calculated by subtracting the absorbance value at 630 nm from the absorbance value at 450 nm.

The affinity constant (K_{aff}) was calculated as follows (Beatty et al. 1987):

$$n = \frac{Ag}{Ag'}; \quad K_{aff} = \frac{n-1}{nAb' - Ab};$$

[Ab] and [Ab′] were the total measurable antibody concentrations in the wells at 1/2 OD_{max} and 1/2 OD'_{max} for plates coated with antigen concentrations of [Ag] and [Ag′], respectively.

CCK-8 Assay

Briefly, HaCaT cells were seeded in 96-well plates at 1×10^3 cells/well and cultured in DMEM medium (Gibco, USA) containing 10% fetal bovine serum (FBS, Gibco, USA) for overnight incubation at 37 °C in 5% CO_2. After 2 h of starvation, cells were treated with 100, 50, 25, 12.5, 6.25, 3.125, 1.563, 0.781 ng/mL of FGF-2 for 48 h to determine the maximum pro-proliferative concentration of FGF-2 on HaCaT cells. To determine the maximum inhibitory concentration of M-F3 ng/mL on the FHCM, FHCM were treated with 100, 25, 6.25, 1.563, 0.391, 0.098, 0.024 ng/mL of M-F3 for 48 h. Finally, 10 μL CCK-8 (Sigma, USA) was added to each well and incubated in the dark for 2 h. The absorbance value was measured at 450 nm using a microplate reader.

Colony Formation Assay

Briefly, HaCaT cells were seeded in 6-well plates at 3×10^3 cells/well and then treated with 25 ng/mL of FGF-2 or 25 ng/mL of FGF-2 and 100 ng/mL of M-F3 in DMEM medium containing 0.2% FBS, respectively. After incubation at 37 °C and 5% CO_2 for 7 days, the cells were fixed

in 4% paraformaldehyde (Guge Biotech, China) for 30 min and then stained with 0.5% crystal violet staining solution (Beyotime, China). After washing in PBS and drying at room temperature, cell colonies were photographed and quantified using a Gel DocTM XR + and Image J software, respectively.

EdU Staining Assay

Briefly, HaCaT cells were seeded in 24-well plates at 1×10^4 cells/well and cultured in DMEM medium containing 10% FBS for overnight incubation at 37 °C in 5% CO_2. After 2 h of starvation, the cells were treated with 25 ng/mL of FGF-2 or 25 ng/mL of FGF-2 and 100 ng/mL of M-F3, respectively. After 48 h of incubation, EdU staining of cells was performed using the BeyoClick™ EdU-488 cell proliferation assay kit (Beyotime, China) according to the manufacturer's instructions. EdU-positive rate (%) = EdU-positive cells (green cells)/total Hoechst-positive cells (blue cells).

Scratch Assay

Briefly, HaCaT cells were seeded in 6-well plates at 1×10^6 cells/well and cultured in DMEM medium containing 10% FBS. After overnight incubation at 37 °C and 5% CO_2, the monolayer cells were scraped in a straight line and washed. After 2 h of starvation, the cells were treated with 25 ng/mL of FGF-2 or 25 ng/mL of FGF-2 and 100 ng/mL of M-F3 for 24 h, respectively. Photographs of the scrapings were taken at 0, 12 and 24 h using an inverted microscope (Olympus, Japan). The area of cell migration was calculated by subtracting the area of the scratch at 12 and 24 h from the area of the scratch at 0 h.

Establishment of the Psoriasis Mice Model

IMQ is a ligand that activates Toll-like receptors on macrophages, monocytes, and plasmacytoid dendritic cells, triggering an inflammatory response (Jiang et al. 2020). Due to its ability to induce psoriasis-like skin features in mice, such as red papules, plaques, scales, and epidermal thickening, IMQ is commonly used to establish psoriasis animal models (Xu et al. 2021). Briefly, an area (2 cm × 3 cm) on the back of male BALB/c mice was shaved. The mice were then randomly divided into four groups including control, IMQ + PBS, IMQ + M-F3, and IMQ + calcipotriol, with each group containing five mice ($n = 5$). 62.5 mg of IMQ was applied daily to the shaved back of each mouse separately for 6 days, except for the control group. Six hours after each application of IMQ, the mice were treated with PBS as vehicle control and 20 mg/kg of M-F3 by subcutaneous injection administration. Calcipotriol treatment was performed according to the manufacturer's instructions. The Psoriasis Area Severity Index (PASI) was scored in terms of erythema, infiltration and scales on a scale of 0 to 4 points (0, none; 1 and 2, moderate; 3, severe; 4, very severe). The cumulative score was calculated as erythema plus infiltration plus scales scores.

Flow Cytometry, Histological and Immunohistochemical Analysis

Mice were euthanized on day 7. Analysis of neutrophil infiltration in skin lesions was performed using a FACS-Calibur flow 172 cytometer (Becton–Dickinson, San Jose, CA, USA). For histological analysis, skin lesion tissues were fixed in 4% paraformaldehyde for 24 h and then embedded in paraffin. The treated tissues were continued to section at 4 μm thickness and stained with hematoxylin and eosin (H&E). Skin sections were further incubated with primary anti-Ki67 antibody overnight. HRP-conjugated secondary antibody and 3,3′-diaminobenzidine (DAB) substrate were used to develop Ki67 immunoreactivities for immunohistochemical analysis.

Quantitative Real-Time PCR

Total RNA from skin lesions was extracted using RNAiso reagent (Takara, Japan) according to the manufacturer's instructions. Reverse transcription of total RNA was performed using the PrimeScript™ RT reagent kit with gDNA Eraser (Takara, Japan) for quantitative real-time (qRT)-PCR analysis of IL-1β, IL-6, IL-23, TNF-α, CXCL1, and CXCL20 mRNA levels. GAPDH was used as the internal reference gene. The primer sequences used for qRT-PCR were listed in Table 1.

Statistical Analysis

All data were presented as mean ± SD ($n = 3$ or 5). Statistical analysis was carried out using GraphPad Prism 7.0 software. Statistical differences were determined by using one-way ANOVA. The statistically significant P values were indicated by asterisks ($^*p < 0.05$, $^{**}p < 0.01$, $^{***}p < 0.001$), and ns was considered as no significance.

Results

Construction, Expression, Purification, and Characterization of M-F3

In a previous study, we found that the *E. coli* expression system resulted in a limited yield of approximately 2.5 mg of recombinant F3 from 1 L of induced bacterial lysates. To overcome this limitation, we explored alternative

Table 1 The primers for qRT-PCR

Primers	Sequences (5′–3′)
GAPDH (F)	CCCTTAAGAGGGATGCTGCC
GAPDH (R)	ACTGTGCCGTTGAATTTGCC
IL-1β (F)	GAGCACCTTCTTTTCCTTCATCTT
IL-1β (R)	TCACACACCAGCAGGTTATCATC
IL-6 (F)	CCTCTCTGCAAGAGACTTCCAT
IL-6 (R)	AGTCTCCTCTCCGGACTTGT
IL-23 (F)	CAAAGGATCCGCCAAGGTCT
IL-23 (R)	CTTGCCCTTCACGCAAAACA
TNF-α (F)	ATCCGCGACGTGGAACTG
TNF-α (R)	ACCGCCTGGAGTTCTGGAA
CXCL1 (F)	GCTGGGATTCACCTCAAGAAC
CXCL1 (R)	AAGGGAGCTTCAGGGTCAAG
CCL20 (F)	ATCTGTGTGCGCTGATCCAA
CCL20 (R)	CCCCCATGGATTGTGGGAAA

The (F) and (R) denoted the forward primer and reverse primer

expression systems and decided to use the *P. pastoris* due to its ability to produce gram amounts of recombinant protein per litre of culture (Ahmad et al. 2014). Notably, post-translational modifications, such as N-glycosylation, that occur in expressed proteins in *P. pastoris* may have potentially unfavorable effects on protein yield, functional activity, and immunogenicity (Hoshida et al. 2013; Peng et al. 2009; Wang et al. 2000). Therefore, we used the NetNGlyc 1.0 online server to determine putative N-glycosylation sites in the F3 amino acid sequence. A putative N-glycosylation site at position 25 (asparagine; N25) was identified and substituted with glutamine (Q25) by site-directed mutagenesis to construct M-F3. The amino acid sequence of M-F3 was fused to a 6 × His tag at the C-terminus to improve its purification efficiency and inserted into the eukaryotic expression plasmid pPICZα A. The schematic diagram of the construction was shown in Fig. 1a.

To determine the expression of M-F3 in *P. pastoris*, GS115 strains were transformed with recombinant pPICZα A-M-F3 or blank pPICZα A as a negative control, respectively. SDS-PAGE and immunoblotting analyses showed that M-F3 was mainly expressed in the secreted form, and no targeted band was seen in the cell precipitation or negative control (Fig. 1b). The induced cell supernatant containing M-F3 was subjected to Ni–NTA affinity chromatography. Some endogenously secreted host proteins failed to bind Ni–NTA in PBS buffer containing 0–100 mM imidazole. The fraction of M-F3 eluted by 300 mM imidazole was analyzed by SDS-PAGE followed by Coomassie brilliant blue staining to determine the purity (Fig. 1c), and then quantified by using the BCA protein assay kit. In the end, about 40 mg of M-F3 with more than 95% purity was obtained in 1 L of fermentation medium.

Since PNGase F readily cleaves the N-linked oligosaccharides in glycoproteins, it has been widely used to analyze protein glycosylation (Kovács et al. 2022). Recombinant F3 and M-F3 isolated from *P. pastoris* were treated with PNGase F to analyze protein glycosylation. SDS-PAGE analysis showed that only one targeted band and no molecular weight reduction was observed when M-F3 was treated with or without PNGase F, whereas a single band appeared only after F3 was treated with PNGase F (Fig. 1d).

The specificity of M-F3 was determined by comparison with cross-reactivity with different antigens according to the ELISA assay. As shown in Fig. 1e, the OD value of M-F3 binding to FGF-2 was significantly higher than that of other unrelated antigens. The affinity constant (K_{aff}) refers to the binding capacity of the antibody to the antigen, and the valuable Nbs with their high-affinity constant typically ranged between 10^7 and 10^{12} L/mol (Zhang et al. 2020). The K_{aff} of M-F3 was calculated as $(7.49 \pm 1.53) \times 10^8$ L/mol according to the non-competitive ELISA assay (Fig. 1f).

M-F3 Inhibits Proliferation and Migration in FGF-2-Induced HaCaT Cell Model

As mentioned above, FGF-2 acts as a mitogen for keratinocytes, and its positive immunoreactivity has been detected in the basal layer of psoriatic lesions. Therefore, the FHCM can recapitulate the key feature of keratinocyte overproliferation in psoriasis. Stimulation of HaCaT cells with FGF-2 at a concentration of 25 ng/mL for 48 h showed maximal pro-growth effects, resulting in a 1.41-fold increase in cell proliferation compared to the control group (Fig. 2a). This concentration was therefore chosen to establish the FHCM. This model was then used to evaluate the specific effects of M-F3 on the hyperproliferative phenotype of psoriatic keratinocytes by interfering with FGF-2-mediated mitogenic signaling.

The CCK-8 assay showed that M-F3 effectively inhibited FHCM proliferation in a concentration-dependent manner at 48 h, with the maximum cell growth inhibition rate reaching 58.04% at a concentration of 100 ng/mL (Fig. 2b). In subsequent experiments, FHCM was consistently treated with 100 ng/mL of M-F3. The colony formation assay is a useful tool for assessing the proliferative potential of individual cells. As shown in Fig. 2c, f, the mean cell clone numbers were reduced by 1.26-fold in the FHCM + M-F3 group compared to the FHCM group. EdU (5-ethynyl-2′-deoxyuridine) is a novel thymidine analogue that can be incorporated into newly synthesized DNA during DNA synthesis as a substitute for thymidine (Sun et al. 2016). It is therefore used to assess cell proliferation. As shown in Fig. 2d, g, the rate of EdU-positive cells in the FHCM group was significantly reduced from 37.72 to 20.68% after treatment with M-F3, indicating that M-F3 effectively inhibited the DNA synthesis

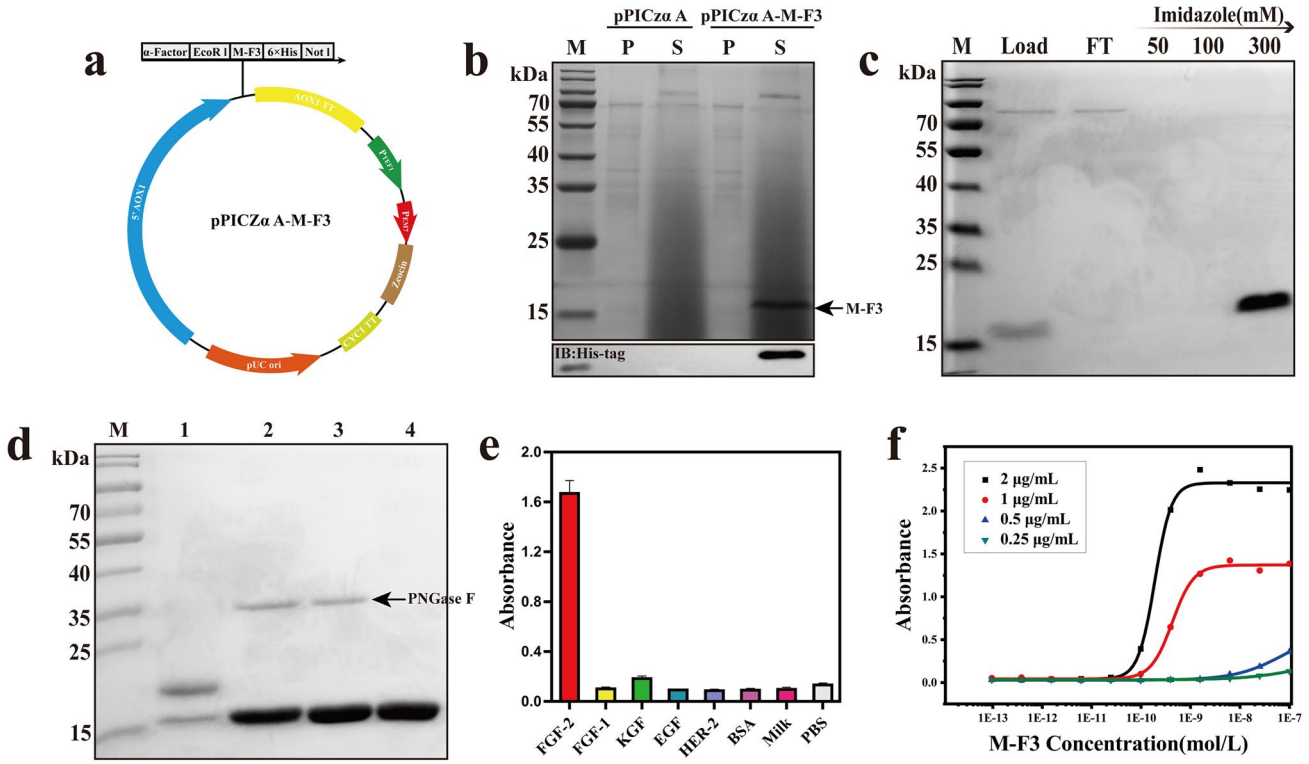

Fig. 1 Construction, expression, purification, and characterization of M-F3. **a** Schematic diagram of the construction of the pPICzα A-M-F3 expression vector. **b** Recombinant expression of M-F3 in *P. pastoris* was analyzed by SDS-PAGE followed by Coomassie brilliant blue staining. Lane M, protein molecular weight marker; lane P, total induced cell pellet; lane S, total induced cell supernatant. **c** Ni–NTA affinity chromatography of recombinant M-F3 was analyzed by SDS-PAGE followed by Coomassie brilliant blue staining. Lane Load, total induced cell supernatant containing M-F3; lane FT, unbound protein; lane 4–6, the fractions eluted by 50, 100, and 300 mM imidazole. **d** Identification of N-glycosylation sites in recombinant M-F3 was analyzed by SDS-PAGE followed by Coomassie brilliant blue staining. Lane 1, purified F3 treated with PBS; lane 2, purified F3 treated with PNGase F; lane 3, purified M-F3 treated with PNGase F; lane 4, purified M-F3 treated with PBS. **e** Specificity analysis of M-F3. **f** Affinity analysis of M-F3

capacity of FHCM. Furthermore, FGF-2 stimulation was found to promote the migration of HaCaT cells, with a 1.38-fold and 1.58-fold increase in the migration rate at 12 and 24 h, respectively, compared to the control group. However, in the presence of M-F3, this promotion was partially inhibited (Fig. 2e, h, i).

M-F3 Attenuates the Severity of IMQ-Induced Psoriasis-Like Skin Lesions in Mice

The IMQ-induced psoriasis-like mouse model was used to further evaluate the therapeutic potential of M-F3. In the in vivo study on days 0–7 (Fig. 3a), IMQ-treated mice exhibited psoriasis-like lesions characterized by red papules, plaques, and scaling, indicating successful establishment of the psoriasis-like mouse model. Treatment with PBS had no ameliorating effect on these features, but treatment with M-F3 and calcipotriol effectively improved the skin conditions (Fig. 3b). Epidermal thickening is another characteristic feature of psoriasis. As expected, histopathological analysis in Fig. 3c showed a significant increase in epidermal thickness following IMQ stimulation compared to normal skin. In contrast, IMQ-induced mice treated with M-F3 and calcipotriol showed a 2.87- and 2.38-fold decrease in epidermal thickness, respectively. In addition, a significant increase in the spleen index was observed in the IMQ + PBS group compared to the control group. However, in IMQ-induced mice treated with M-F3 and calcipotriol, splenic hypertrophy was effectively attenuated, resulting in a 1.49- and 1.64-fold reduction in the spleen index, respectively (Fig. 3d).

To determine whether M-F3 treats psoriasis by inhibiting FGF-2-mediated active proliferation of epidermal keratinocytes, PASI scores and Ki67 immunohistochemical analysis were also performed. The cumulative scores (erythema plus infiltration plus scales scores) of IMQ-induced mice treated with M-F3 and calcipotriol were lower than those of IMQ + PBS treatment on day 7 (Fig. 3e). Ki67 is widely used as a proliferation marker to determine the cell growth fraction. As shown in Fig. 3f, positive immunoreactivity for Ki67 in the basal and spinous layers of psoriatic lesions was significantly attenuated by M-F3 and calcipotriol

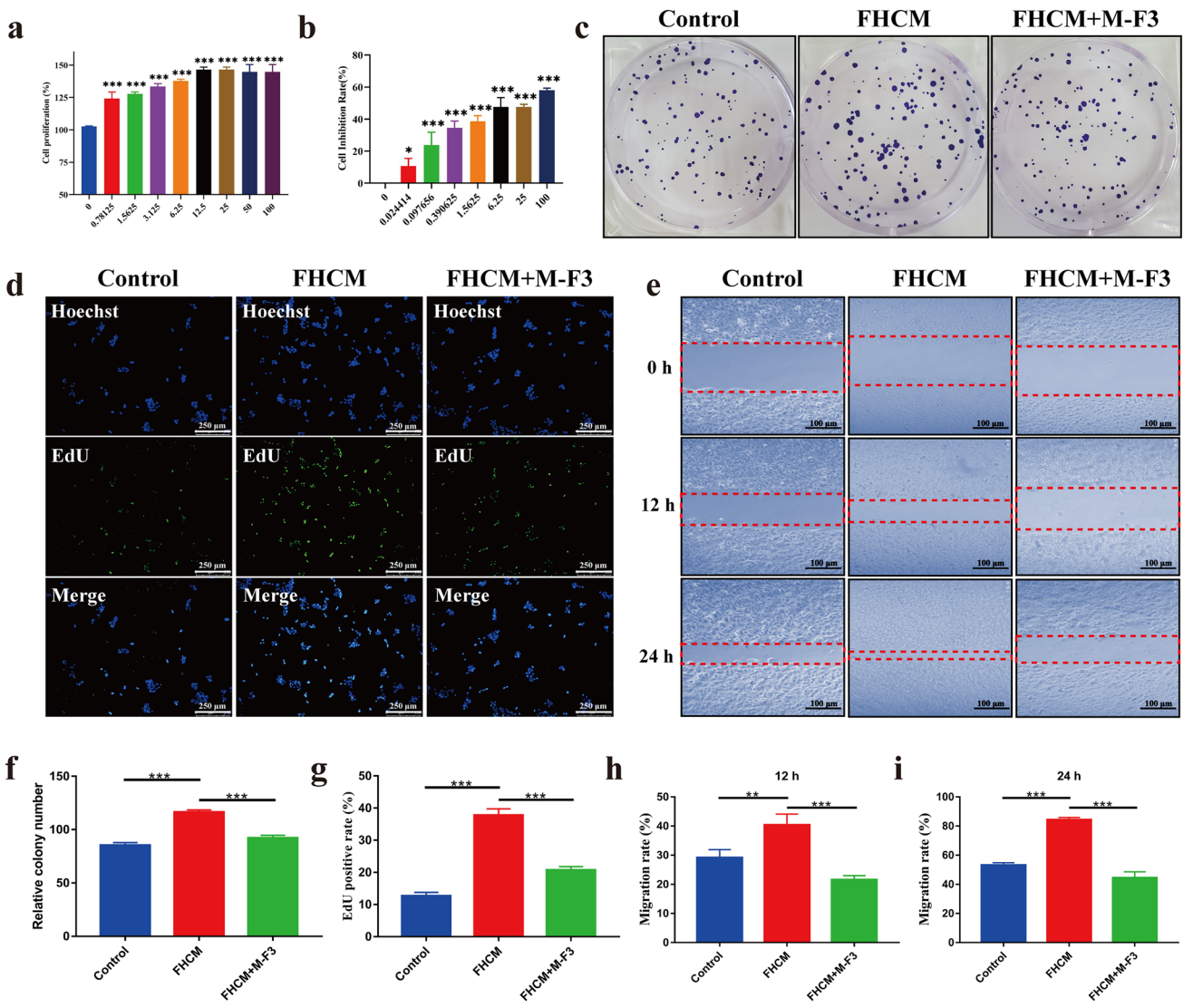

Fig. 2 Effect of M-F3 on proliferation and migration in FHCM. **a** The proliferative effect of FGF-2 on HaCaT cells was determined by CCK-8 assay. **b**, **c** Cell proliferation inhibition of FHCM treated with M-F3 was measured by CCK-8 and clonogenic cell proliferation assays. **d** Effect of M-F3 on the DNA synthesis capacity of FHCM was determined by EdU staining assay. **e** Effect of M-F3 on the migration capacity of FHCM for 12 h and 24 h was determined by scratch assay. **f** Statistics of the number of cell clones corresponding to **c**. **g** The calculation of EdU positive rate corresponding to **d**. **h**, **i** The calculation of migration rate for 12 h and 24 h corresponding to **e**. $^{**}p < 0.01$, $^{***}p < 0.001$, compared to FHCM group

treatment (2.19- and 1.77-fold reduction in Ki67 expression, respectively).

M-F3 Ameliorates the Inflammatory Microenvironment in IMQ-Induced Psoriasis-Like Skin Lesions in Mice

To further investigate the potential of M-F3 to attenuate IMQ-induced skin inflammation, we examined the mRNA levels of relevant inflammatory cytokines (IL-1β, IL-6, IL-23, and TNF-α) and chemokines (CXCL1 and CCL20) in the skin lesions using qRT-PCR. As expected, the mRNA levels of IL-1β, IL-6, IL-23, TNF-α, CXCL1, and CCL20 were significantly increased in the skin lesions compared to normal skin (Zhou et al. 2022). In contrast, M-F3 and calcipotriol effectively inhibited IMQ-induced upregulation of these inflammatory cytokines and chemokines (Fig. 4a). In addition, according to the flow cytometry results in Fig. 4b, the percentage of infiltrating neutrophils in the psoriatic lesions was reduced from 46.20% to 8.51% and 7.83% after treatment with M-F3 and calcipotriol, respectively.

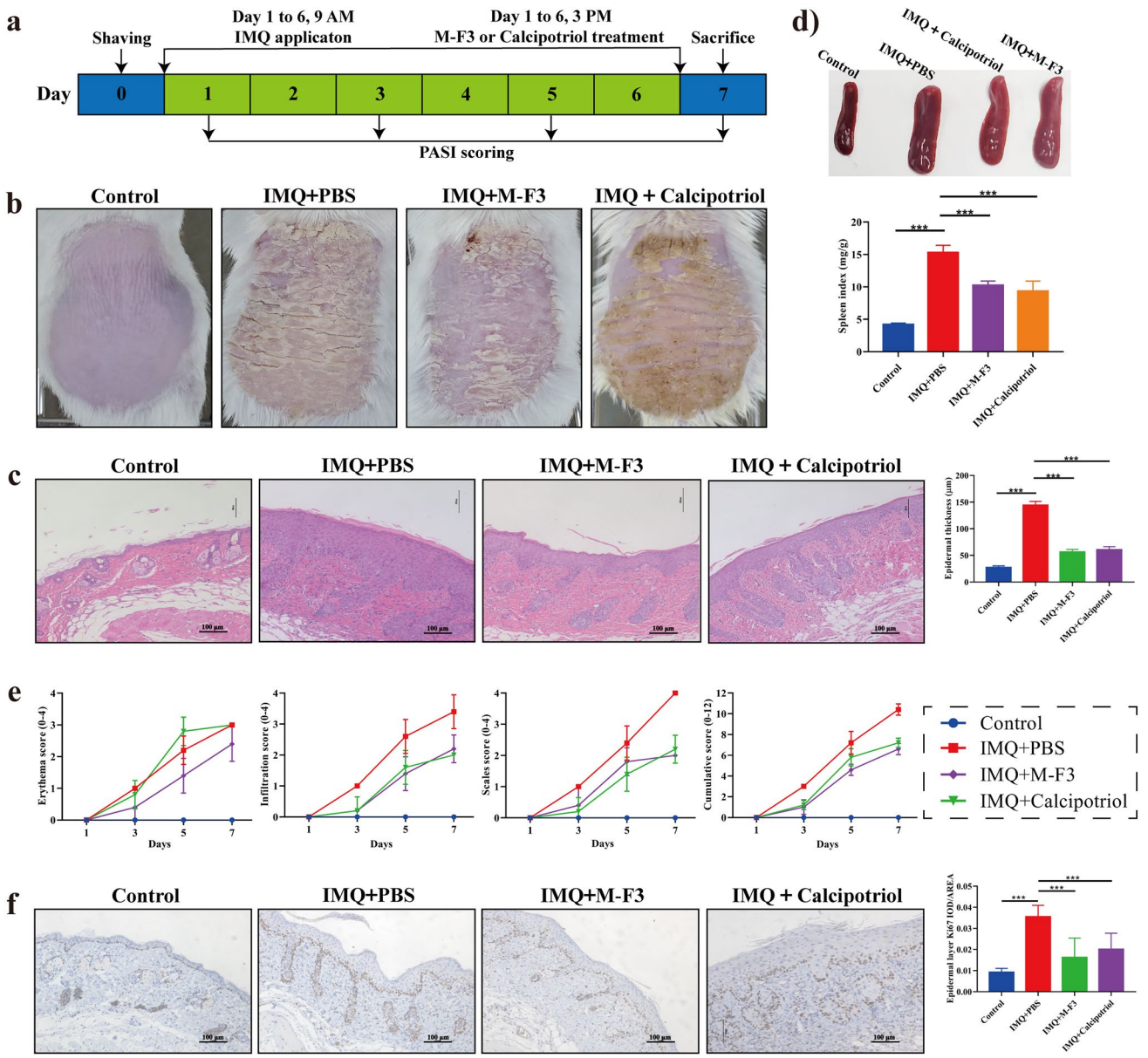

Fig. 3 Effect of M-F3 on the IMQ-induced psoriasis-like mouse model. **a** Schematic diagram showing the experimental design and procedure for in vivo treatment of mice. **b** Pathological symptoms in each group on day 7. **c** H&E staining. **d** Spleen index of each group on day 7. **e** Erythema, infiltration, and scales were scored by PASI on days 1, 3, 5, and 7. **f** Immunohistochemical staining for Ki67. Image-pro Plus 6.0 software was used to calculate the epidermal thickness and quantify the average optical density (AOD) of Ki67 in skin sections. AOD = IOD/Area. ***$p < 0.001$, compared with the IMQ group

Discussion

Nbs, a single-domain antibody, are considered to be the next generation of antibody derivatives (Liu et al. 2021). A number of Nbs have entered clinical trials due to their superior properties (natural origin, small size, low immunogenicity, high antigen binding affinity, stability, and water solubility) (Jovčevska and Muyldermans 2020). For example, an anti-IL-17A/F Nb (M1095) has favorable biosafety and dose-dependent efficacy in psoriasis patients (Svecova et al. 2019), demonstrating the potential of using Nbs to immunotarget cytokines for the treatment of psoriasis. In previous work, our laboratory had successfully screened a biologically active F3 using phage display technology. However, the low yield of F3 produced in the *E. coli* expression system limits its availability. To overcome this, we turned to the *P. pastoris* expression system. *P. pastoris*, an engineered methylotrophic yeast, has emerged as a promising choice in the biopharmaceutical field due to its ability to achieve high cell density growth and excellent secretion of heterologous

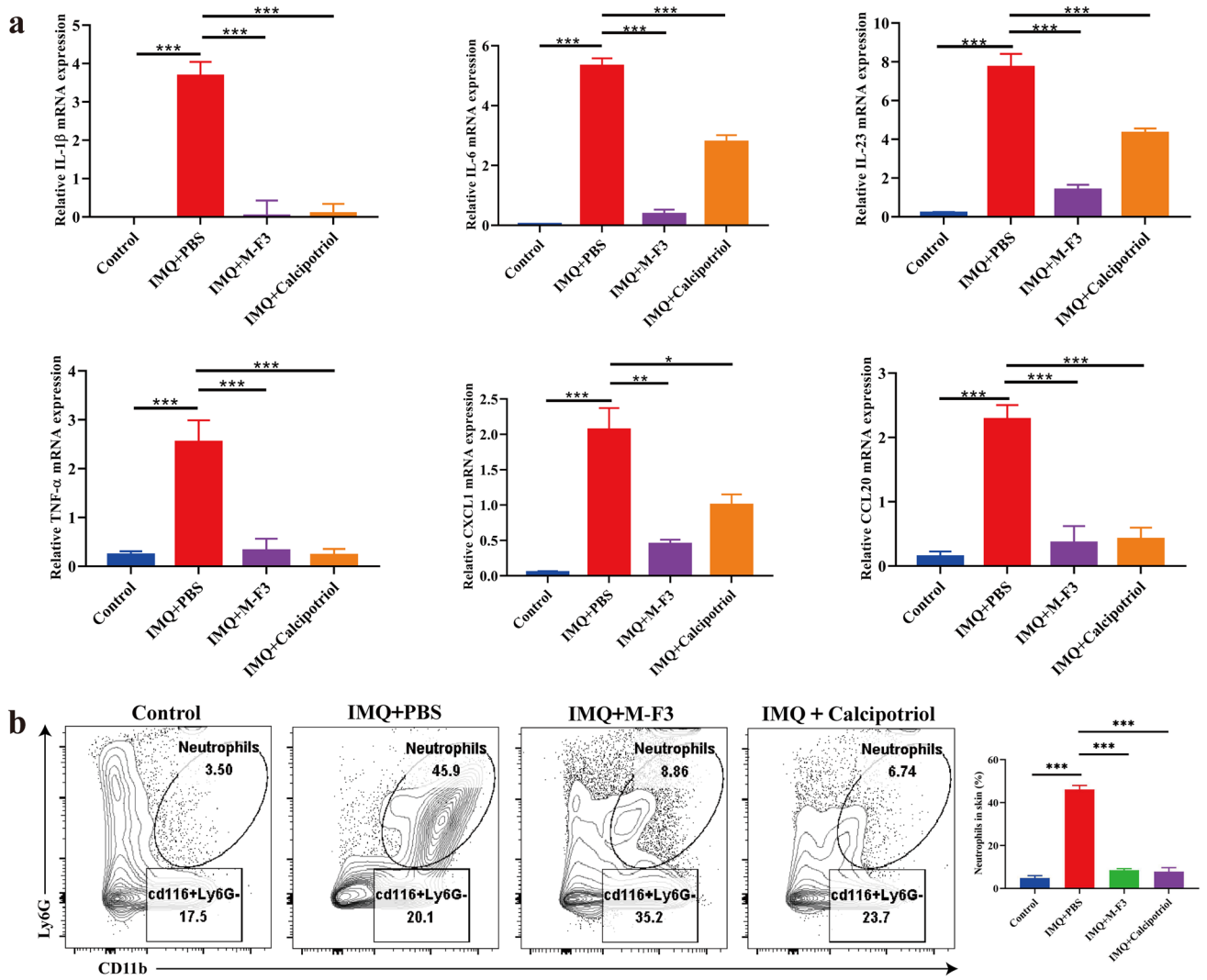

Fig. 4 Effect of M-F3 on the inflammatory microenvironment in IMQ-induced psoriasis-like skin lesions. **a** The mRNA levels of IL-1β, IL-6, IL-23, TNF-α, CXCL1, and CCL20 were measured by qRT-PCR in skin lesions, respectively. **b** The levels of neutrophil infiltration in the skin lesions were determined by flow cytometry. $^{*}p<0.05$, $^{**}p<0.01$, $^{***}p<0.001$, compared with the IMQ + PBS group

proteins with minimal fermentation medium (Cos et al. 2006). Baghban et al. (2016) reported that the final production of camelid Nb against *Clostridium botulinum* neurotoxin E produced in *P. pastoris* was higher than that of the *E. coli* expression system. In addition, the *P. pastoris* expression system offers the advantage of simplified purification of recombinant proteins, as it shows minimal production of endogenous secreted proteins (Han et al. 2020). These characteristics make *P. pastoris* a well-suited expression system for industrial-scale production of recombinant proteins. However, as also mentioned above, post-translational modifications such as N-glycosylation may have an unfavorable effect on the yield, functional activity, and immunogenicity of the target protein. Therefore, we constructed, expressed and isolated de-glycosylated M-F3 in *P. pastoris* (Fig. 1a–c). As expected, we obtained approximately 40 mg of M-F3 with over 95% purity in 1 L of fermentation medium, representing a 16-fold increase in yield compared to the *E. coli* expression system. We further identified M-F3 as a non-N-glycosylated protein using PNGase F (Fig. 1d). Finally, we tested the specificity and affinity of M-F3 and found that it had sufficient specificity and binding capacity to meet the therapeutic needs of FGF-2-related diseases (Fig. 1e, f).

Keratinocytes are a type of skin resident cell, and their hyperproliferation is one of the main features of psoriatic lesions. Members of the FGFR family play a central role in the regulation of the epidermal keratinocyte proliferation (Werner and Smola 2001). For example, Xiao et al. (2020) proposed that overexpression of FGFR2 in keratinocytes may contribute to keratinocyte overproliferation and the

development of psoriasis. In addition, FGF-7, a specific ligand for FGFR2, is overexpressed in the basal epidermal cell layer of transgenic mice, resulting in epidermal hyperplasia. Notably, FGF-2, which also functions as a specific ligand for FGFR2, is positively immunoreactive in the basal layer of psoriatic lesions as mentioned above. Therefore, M-F3 may inhibit the associated activation of mitogenic signaling triggered by FGF-2/FGFR binding in psoriatic keratinocytes. On this basis, we established the FHCM, which mimics the key feature of keratinocyte overproliferation in psoriasis. Although FHCM does not fully recapitulate all aspects of psoriasis, it provides a valuable in vitro tool for studying the effects of anti-proliferative and anti-migratory agents on psoriatic keratinocytes. As expected, M-F3 inhibited the proliferation and migration of FHCM (Fig. 2). However, further experiments on the FGF-2-mediated mitogenic signaling pathway are required to support these results.

To further validate the therapeutic potential of M-F3 in psoriasis, we performed in vivo experiments (Fig. 3a). IMQ, an agonist of Toll-like receptor 7/8 ligands, was originally used for topical therapy of genital and perianal warts caused by human papillomavirus (Kuang et al. 2018). However, IMQ was unexpectedly found to induce psoriasis-like lesions characterized by red papules, plaques, scales, and epidermal thickening in mice (Van Belle et al. 2012; van der Fits et al. 2009). It is therefore now widely used to establish a psoriasis-like mouse model. Interestingly, M-F3 treatment ameliorated the aforementioned symptoms in IMQ-induced mice, showing a therapeutic effect similar to that of calcipotriol treatment (Fig. 3b, c). The spleen, the largest secondary lymphoid organ in the immune system, reflects the level of immunity in the organism (Tang et al. 2022a). In IMQ-treated mice, the spleen is enlarged, indicating systemic immune activation (Jabeen et al. 2020). M-F3 significantly inhibited the IMQ-induced upregulation of immune response levels in mice (Fig. 3d). PASI scores and skin Ki67 immunoreactivity positively correlated with epidermal keratinocyte proliferation. The significant upregulation of PASI scores reflects the abnormal proliferation and higher mitotic state of epidermal keratinocytes. In normal skin, Ki67, a marker of tissue cell proliferation and growth, is expressed at low levels. Shi et al. (2019) reported that oxymatrine regulated mitosis and inhibited Ki-67 overexpression in skin lesions, resulting in improvement of psoriatic lesions. This is similar to our results, in which epidermal keratinocyte proliferation in psoriatic skin was inhibited by M-F3 through downregulation of PASI scores and Ki67 expression to restore skin homeostasis (Fig. 3e, f).

There is increasing evidence that keratinocytes play a pivotal role in the maintenance of psoriasis (Harper et al. 2009). Briefly, overproliferating keratinocytes in psoriatic lesions produce IL-23, which is sufficient to activate IL-17-producing immune cells to secrete the inflammatory mediator IL-17 (Li et al. 2018). This in turn binds to receptors on keratinocytes via various cellular signaling pathways, inducing them to produce chemokines (CXCL1, CXCL8, and CCL20), inflammatory cytokines (IL-1β, IL-6, and TNF-α), and antimicrobial peptides that recruit neutrophils, macrophages, or more Th1 and Th17 cells to sites of inflammation (Zhou et al. 2022). These cells further contribute to the maintenance of the inflammatory cascade response. Moos et al. (2019) also showed that IL-17RA was deleted in various cell types (including T cells, neutrophils, macrophages, or keratinocytes) in transgenic mice. They then observed that inhibition of IL-17RA signaling in T cells, neutrophils, or macrophages did not significantly improve psoriasis-like inflammation in IMQ-treated mice. In contrast, mice with specific deletion of IL-17RA in keratinocytes were largely protected from the inflammatory response (Garzorz-Stark and Eyerich 2019; Moos et al. 2019). Therefore, attenuation of keratinocyte overproliferation may effectively regulate the inflammatory microenvironment at the lesions. As expected, M-F3 treatment significantly downregulated the expression of IL-1β, IL-6, IL-23, TNF-α, CXCL1, and CCL20 mRNA levels in skin lesions as measured by qRT-PCR (Fig. 4a). Although we did not measure the changes in CXCL8 mRNA expression levels in skin lesions after M-F3 treatment, we observed in Fig. 4b that M-F3 effectively inhibited the massive aggregation of neutrophils in the skin lesions. This is because CXCL8 has been shown to contribute to the intraepidermal recruitment of neutrophils (Albanesi et al. 2005). Tang et al. (2022b) had shown that KdPT was effective in downregulating Ki67 expression in skin lesions, accompanied by the alleviation of IMQ-induced dermatitis in mice, which was similar to our findings in Fig. 4.

In conclusion, we have successfully improved the production of anti-FGF-2 Nb and demonstrated its ability to inhibit the aberrant proliferation of keratinocytes in both in vivo and in vitro experiments. These effects alleviated IMQ-induced psoriasis-like inflammation to restore the skin homeostasis. Importantly, our work is significant as there are currently no drugs available that directly target the FGF-2/FGFR axis for the treatment of psoriasis. Instead, the mainstream approach relies on small molecule drugs and antibodies that target inflammatory molecules or pathways. However, further extensive, systematic, and in-depth studies are necessary before this therapy can be used clinically. Specifically, more experiments are required to elucidate the role of the FGF-2/FGFR axis in the pathogenesis of psoriasis. Large-scale clinical trials are also essential to demonstrate the safety, efficacy, and feasibility of this treatment.

Acknowledgements This work was supported by the Special Project for Research and Development in Key areas of Guangdong Province, "Green Biomanufacturing" Key Special Project (Grant No. 2022B1111070007).

Author Contributions SX, HZ, and BXL conceived and designed experiments. ZLZ, JT, KTL, and SLW performed the experiments. ZLZ, BXL, and JT analyzed the data. ZLZ, BXL, and MJT wrote and revised the paper. SX was responsible for study supervision. All authors approved the final manuscript.

Data Availability The datasets used and analyzed in the present study are available from the corresponding author on reasonable request.

Declarations

Conflict of interest The authors declared no competing interests.

Consent for Publication Not applicable.

Ethical Approval All animal experiments were approved by the Animal Ethical Committees of Jinan University, Guangzhou, China.

References

Ahmad M, Hirz M, Pichler H et al (2014) Protein expression in *Pichia pastoris*: recent achievements and perspectives for heterologous protein production. Appl Microbiol Biotechnol 98:5301–5317. https://doi.org/10.1007/s00253-014-5732-5

Albanesi C, Scarponi C, Giustizieri M et al (2005) Keratinocytes in inflammatory skin diseases. Curr Drug Targets Inflamm Allergy 4:329–334. https://doi.org/10.2174/1568010054022033

Amin M, No DJ, Egeberg A et al (2018) Choosing first-line biologic treatment for moderate-to-severe psoriasis: What does the evidence say? Am J Clin Dermatol 19:1–13. https://doi.org/10.1007/s40257-017-0328-3

Andrys C, Borska L, Pohl D et al (2007) Angiogenic activity in patients with psoriasis is significantly decreased by Goeckerman's therapy. Arch Dermatol Res 298:479–483. https://doi.org/10.1007/s00403-006-0723-8

Armstrong AW, Read C (2020) Pathophysiology, clinical presentation, and treatment of psoriasis: a review. JAMA 323:1945. https://doi.org/10.1001/jama.2020.4006

Baghban R, Gargari SLM, Rajabibazl M et al (2016) Camelid-derived heavy-chain nanobody against *Clostridium botulinum* neurotoxin E in *Pichia pastoris*: Nanobody against *Clostridium botulinum* neurotoxin E. Biotechnol Appl Biochem 63:200–205. https://doi.org/10.1002/bab.1226

Battaglin F, Puccini A, Ahcene Djaballah S et al (2019) The impact of panitumumab treatment on survival and quality of life in patients with RAS wild-type metastatic colorectal cancer. Cancer Manag Res 11:5911–5924. https://doi.org/10.2147/CMAR.S186042

Beatty JD, Beatty BG, Vlahos WG (1987) Measurement of monoclonal antibody affinity by non-competitive enzyme immunoassay. J Immunol Methods 100:173–179. https://doi.org/10.1016/0022-1759(87)90187-6

Chen C-H, Poucher S, Lu J et al (2004) Fibroblast growth factor 2: from laboratory evidence to clinical application. Curr Vasc Pharmacol 2:33–43. https://doi.org/10.2174/1570161043476500

Cos O, Ramón R, Montesinos JL et al (2006) Operational strategies, monitoring and control of heterologous protein production in the methylotrophic yeast *Pichia pastoris* under different promoters: a review. Microb Cell Fact 5:17. https://doi.org/10.1186/1475-2859-5-17

Dailey L, Ambrosetti D, Mansukhani A et al (2005) Mechanisms underlying differential responses to FGF signaling. Cytokine Growth Factor Rev 16:233–247. https://doi.org/10.1016/j.cytogfr.2005.01.007

Ferrara N (1999) Role of vascular endothelial growth factor in the regulation of angiogenesis. Kidney Int 56:794–814. https://doi.org/10.1046/j.1523-1755.1999.00610.x

Gao J, Chen F, Fang H et al (2020) Daphnetin inhibits proliferation and inflammatory response in human HaCaT keratinocytes and ameliorates imiquimod-induced psoriasis-like skin lesion in mice. Biol Res 53:48. https://doi.org/10.1186/s40659-020-00316-0

Garzorz-Stark N, Eyerich K (2019) Psoriasis pathogenesis: keratinocytes are back in the spotlight. J Invest Dermatol 139:995–996. https://doi.org/10.1016/j.jid.2019.01.026

Han LK, Oanh NCK, Nghia NH et al (2020) Secretory expression of the recombinant FGF-2 protein in *Pichia pastoris* carrying multiple copies of target gene. VNUHCM J Sci Technol Dev 23:499–507. https://doi.org/10.32508/stdj.v23i2.1746

Harper EG, Guo C, Rizzo H et al (2009) Th17 cytokines stimulate CCL20 expression in keratinocytes in vitro and in vivo: implications for psoriasis pathogenesis. J Invest Dermatol 129:2175–2183. https://doi.org/10.1038/jid.2009.65

Haugh I, Preston A, Kivelevitch D et al (2018) Risankizumab: an anti-IL-23 antibody for the treatment of psoriasis. Drug Des Devel Ther 12:3879–3883. https://doi.org/10.2147/DDDT.S167149

Hoshida H, Fujita T, Cha-aim K et al (2013) N-glycosylation deficiency enhanced heterologous production of a *Bacillus licheniformis* thermostable α-amylase in *Saccharomyces cerevisiae*. Appl Microbiol Biotechnol 97:5473–5482. https://doi.org/10.1007/s00253-012-4582-2

Hu Y, Liu C, Muyldermans S (2017) Nanobody-based delivery systems for diagnosis and targeted tumor therapy. Front Immunol 8:1442. https://doi.org/10.3389/fimmu.2017.01442

Jabeen M, Boisgard A-S, Danoy A et al (2020) Advanced characterization of imiquimod-induced psoriasis-like mouse model. Pharmaceutics 12:789. https://doi.org/10.3390/pharmaceutics12090789

Jiang B-W, Zhang W-J, Wang Y et al (2020) Convallatoxin induces HaCaT cell necroptosis and ameliorates skin lesions in psoriasis-like mouse models. Biomed Pharmacother 121:109615. https://doi.org/10.1016/j.biopha.2019.109615

Jovčevska I, Muyldermans S (2020) The therapeutic potential of nanobodies. BioDrugs 34:11–26. https://doi.org/10.1007/s40259-019-00392-z

Kijanka M, Dorresteijn B, Oliveira S et al (2015) Nanobody-based cancer therapy of solid tumors. Nanomedicine 10:161–174. https://doi.org/10.2217/nnm.14.178

Kormeili T, Lowe NJ, Yamauchi PS (2004) Psoriasis: immunopathogenesis and evolving immunomodulators and systemic therapies; U.S. experiences. Br J Dermatol 151:3–15. https://doi.org/10.1111/j.1365-2133.2004.06009.x

Kovács N, Farsang R, Szigeti M et al (2022) Enhanced recombinant protein production of soluble, highly active and immobilizable PNGase F. Mol Biotechnol 64:914–918. https://doi.org/10.1007/s12033-022-00464-6

Kuang Y-H, Lu Y, Liu Y-K et al (2018) Topical Sunitinib ointment alleviates Psoriasis-like inflammation by inhibiting the proliferation and apoptosis of keratinocytes. Eur J Pharmacol 824:57–63. https://doi.org/10.1016/j.ejphar.2018.01.048

Landeck L, Sabat R, Ghoreschi K et al (2021) Immunotherapy in psoriasis. Immunotherapy 13:605–619. https://doi.org/10.2217/imt-2020-0292

Ledsgaard L, Ljungars A, Rimbault C et al (2022) Advances in antibody phage display technology. Drug Discov Today 27:2151–2169. https://doi.org/10.1016/j.drudis.2022.05.002

Li H, Yao Q, Mariscal AG et al (2018) Epigenetic control of IL-23 expression in keratinocytes is important for chronic skin inflammation. Nat Commun 9:1420. https://doi.org/10.1038/s41467-018-03704-z

Liu M, Li L, Jin D et al (2021) Nanobody—a versatile tool for cancer diagnosis and therapeutics. Wiley Interdiscip Rev Nanomed Nanobiotechnol 13:e1697. https://doi.org/10.1002/wnan.1697

Moos S, Mohebiany AN, Waisman A et al (2019) Imiquimod-induced psoriasis in mice depends on the IL-17 signaling of keratinocytes. J Invest Dermatol 139:1110–1117. https://doi.org/10.1016/j.jid.2019.01.006

Paz-Ares L, Socinski MA, Shahidi J et al (2016) Correlation of EGFR-expression with safety and efficacy outcomes in SQUIRE: a randomized, multicenter, open-label, phase III study of gemcitabine–cisplatin plus necitumumab versus gemcitabine–cisplatin alone in the first-line treatment of patients with stage IV squamous non-small-cell lung cancer. Ann Oncol 27:1573–1579. https://doi.org/10.1093/annonc/mdw214

Peng A, Gaitonde P, Kosloski MP et al (2009) Effect of route of administration of human recombinant factor VIII on its immunogenicity in hemophilia a mice. J Pharm Sci 98:4480–4484. https://doi.org/10.1002/jps.21765

Salvador J-P, Vilaplana L, Marco M-P (2019) Nanobody: outstanding features for diagnostic and therapeutic applications. Anal Bioanal Chem 411:1703–1713. https://doi.org/10.1007/s00216-019-01633-4

Shi H, Zhou H, Ma A et al (2019) Oxymatrine therapy inhibited epidermal cell proliferation and apoptosis in severe plaque psoriasis. Br J Dermatol 181:1028–1037. https://doi.org/10.1111/bjd.17852

Song H, Pan B, Yi J et al (2014) Featured article: autophagic activation with Nimotuzumab enhanced chemosensitivity and radiosensitivity of esophageal squamous cell carcinoma. Exp Biol Med 239:529–541. https://doi.org/10.1177/1535370214525315

Sun X, Zhang C, Jin H et al (2016) Flow cytometric analysis of T lymphocyte proliferation in vivo by EdU incorporation. Int Immunopharmacol 41:56–65. https://doi.org/10.1016/j.intimp.2016.10.019

Svecova D, Lubell MW, Casset-Semanaz F et al (2019) A randomized, double-blind, placebo-controlled phase 1 study of multiple ascending doses of subcutaneous M1095, an anti-interleukin 17A/F nanobody, in moderate-to-severe psoriasis. J Am Acad Dermatol 81:196–203. https://doi.org/10.1016/j.jaad.2019.03.056

Tang J, Liu C, Liu S et al (2022a) Inhibition of JAK1/STAT3 pathway by 2-methoxyestradiol ameliorates psoriatic features in vitro and in an imiquimod-induced psoriasis-like mouse model. Eur J Pharmacol 933:175276. https://doi.org/10.1016/j.ejphar.2022.175276

Tang J, Zhou Z, Qian J et al (2022b) KdPT alleviates imiquimod-induced psoriasis-like skin lesion in mice via inhibiting proliferation and inflammation response. Pharmazie 77:48–53

Tol J, Punt CJA (2010) Monoclonal antibodies in the treatment of metastatic colorectal cancer: a review. Clin Ther 32:437–453. https://doi.org/10.1016/j.clinthera.2010.03.012

Van Belle AB, de Heusch M, Lemaire MM et al (2012) IL-22 is required for imiquimod-induced psoriasiform skin inflammation in mice. J Immunol 188:462–469. https://doi.org/10.4049/jimmunol.1102224

van der Fits L, Mourits S, Voerman JSA et al (2009) Imiquimod-induced psoriasis-like skin inflammation in mice is mediated via the IL-23/IL-17 axis. J Immunol 182:5836–5845. https://doi.org/10.4049/jimmunol.0802999

Vivanco I, Mellinghoff IK (2010) Epidermal growth factor receptor inhibitors in oncology. Curr Opin Oncol 22:573–578. https://doi.org/10.1097/CCO.0b013e32833edbdf

Wang P, Zhang J, Sun Z et al (2000) Glycosylation of prourokinase produced by *Pichia pastoris* impairs enzymatic activity but not secretion. Protein Expr Purif 20:179–185. https://doi.org/10.1006/prep.2000.1310

Wang L, Zhang G, Qin L et al (2020) Anti-EGFR binding nanobody delivery system to improve the diagnosis and treatment of solid tumours. Recent Pat Anticancer Drug Discov 15:200–211. https://doi.org/10.2174/1574892815666200904111728

Werner S, Smola H (2001) Paracrine regulation of keratinocyte proliferation and differentiation. Trends Cell Biol 11:143–146. https://doi.org/10.1016/S0962-8924(01)01955-9

Wu X, Huang H, Wang C et al (2013) Identification of a novel peptide that blocks basic fibroblast growth factor-mediated cell proliferation. Oncotarget 4:1819–1828. https://doi.org/10.18632/oncotarget.1312

Xiao Y, Wang C, Zeng B et al (2020) miR124-3p/FGFR2 axis inhibits human keratinocyte proliferation and migration and improve the inflammatory microenvironment in psoriasis. Mol Immunol 122:89–98. https://doi.org/10.1016/j.molimm.2020.04.002

Xiong S, Xie Q, Chen C et al (2022) Application of anti-recombinant human basic fibroblast growth factor nanobody. CN Patent CN113150141 B

Xu Y, Zhu J, Hu J et al (2021) L-theanine alleviates IMQ-induced psoriasis like skin inflammation by downregulating the production of IL-23 and chemokines. Front Pharmacol 12:719842. https://doi.org/10.3389/fphar.2021.719842

Yaguchi H, Tsuboi R, Ueki R et al (1993) Immunohistochemical localization of basic fibroblast growth factor in skin diseases. Acta Derm Venereol 73:81–83

Yang EY, Shah K (2020) Nanobodies: next generation of cancer diagnostics and therapeutics. Front Oncol 10:1182. https://doi.org/10.3389/fonc.2020.01182

Zhang C, Zhang W, Tang X et al (2020) Change of amino acid residues in idiotypic nanobodies enhanced the sensitivity of competitive enzyme immunoassay for mycotoxin ochratoxin A in Cereals. Toxins 12:273. https://doi.org/10.3390/toxins12040273

Zhou X, Chen Y, Cui L et al (2022) Advances in the pathogenesis of psoriasis: from keratinocyte perspective. Cell Death Dis 13:81. https://doi.org/10.1038/s41419-022-04523-3

Zittermann SI, Issekutz AC (2006) Basic fibroblast growth factor (bFGF, FGF-2) potentiates leukocyte recruitment to inflammation by enhancing endothelial adhesion molecule expression. Am J Pathol 168:835–846. https://doi.org/10.2353/ajpath.2006.050479